Article ID: 1006-8775(2011) 04-0326-09

INTRASEASONAL OSCILLATIONS IN ASIA TO WESTERN PACIFIC REGION IN BOREAL SUMMER: CONTRASTIVE ANALYSIS FOR ACTIVE AND INACTIVE YEARS OF TROPICAL CYCLONES

HE Jie-lin (何洁琳)[1, 2, 3], WAN Qi-lin (万齐林)[1], GUAN Zhao-yong (管兆勇)[3], LIN Ai-lan (林爱兰)[1], WANG Li-juan (王黎娟)[3]

(1. Guangzhou Institute of Tropical and Marine Meteorology, CMA, Guangzhou 510080 China; 2. Guangxi Climate Center, Nanning 530022 China; 3. Nanjing University of Information Science & Technology, KLME, Nanjing 210044 China)

Abstract: Comparative analysis is carried out by using finite-domain power spectrum and lagged regression methods for the propagating characteristics and air-sea interaction processes of intraseasonal oscillations (ISOs) in the Asia to western Pacific (AWP) region during the boreal summer between the active and inactive tropical cyclone (TC) years from 1979 to 2004. The results show as follows. (1) There exist more significant eastward propagating characteristics of the ISO in the active TC years over the whole AWP region. The ISOs of convection propagate zonally with more eastward extension in the years with active tropical cyclone activities, during which the 20-60-day period is strengthened, western Pacific becomes an area with evident characteristics of the propagation that is closely related to TC activities. (2) The air-sea interaction processes are the same in both active and inactive TC years, and the energy exchanges between the air and the sea play a role in maintaining the northwestward propagation of ISOs. (3) The air-sea interaction is more intensive in the active TC years than in the inactive ones. It is particularly true for the latent heat release by condensation as the result of convection, which may be one of the reasons resulting in significant differences in characteristics of ISOs between the active and inactive TC years.

Key words: intraseasonal oscillation; finite-domain wavenumber-frequency energy spectrum; lagged linear regression; tropical cyclones

CLC number: P444 **Document code:** A **doi:** 10.3969/j.issn.1006-8775.2011.04.002

1 INTRODUCTION

The present researches have indicated that the boreal summer intraseasonal oscillation (ISO) has pronounced geographical characteristics and seasonality, and the Indian Ocean and western Pacific are the two main areas where the ISO convection is most active. The ISO convection propagates eastward with a 30-60-day period in the equatorial region, while prominently northwestward in the western North Pacific and the late summer from August to October[1-7]. The ISO formation mechanisms have been investigated after the low-frequency phenomenon was detected in the early 1970s. It is thought that the external force, feedback of cumulus convection heat, atmospheric nonlinear interaction and the influence of Earth's rotation are the four basic kinetic factors that induce the ISO formations. The Wave-CISK theory, which is based on the cumulus convection heat feedback, and the high-frequency instability coupled Kelvin-Rossby wave theory, which is a result of the boundary layer air-sea interaction, are currently the two main mechanisms to explain the propagation of the ISO[8-19].

The activity of tropical cyclones (TCs) is closely related to the ISO in the boreal summer. Hartmann et al.[20] found that there exists a pronounced 20-25-day period in the western Pacific during September–December which might result from the coupling between large-scale motion and latent heat release on much smaller scales, and the oscillation is closely related to the occurrence of TCs. More TCs form and develop in the MJO wet phase in the western Pacific, during which continued strong westerly and active convection benefit the formation

Received 2010-08-21; **Revised** 2011-07-29; **Accepted** 2011-10-15

Foundation item: Natural Development and Plan for Key Fundamental Research (2009CB421505); National Natural Science Foundation (40775058; 41075073); Tropical Marine & Meteorological Science Foundation (201103); Natural Science Foundation of Guangxi (2010GXNSFA013010)

Biography: HE Jie-lin, Senior engineer, primarily undertaking research on typhoons and monsoons.

Corresponding author: WAN Qi-lin, e-mail: qlwan@grmc.gov.cn

and development of TCs[21-23], while the air-sea interaction, which is closely associated with the TC activities, may have an impact on the ISO[24, 25]. Therefore, although the TC or tropical synoptic waves are modulated by the ISO scale, there may be a feedback on the ISO when the cluster formation of TCs can reach a certain magnitude on the temporal and spatial scales.

To better understand the relationship of TC activities and the ISO, in particular, the impact of TC activities on the ISO, features of ISO convection propagation and air-sea interaction processes between the active and inactive TC years will be examined.

2 DATA AND METHODOLOGY

The datasets used in this study include daily average outgoing longwave radiation (OLR) from the National Oceanic and Atmospheric Administration (NOAA, U.S.A.) and the daily average reanalysis fields from the National Centers for Environmental Protection/National Center for Atmospheric Research (NCEP/NCAR, U.S.A.) with 2.5° ×2.5° grid space and covering the period from 1979 to 2004; wind, temperature, specific humidity and the air-sea interaction parameters, surface latent heat flux (SLHF), skin temperature (SKT) and surface downward shortwave radiative flux (DSWRF)[26]; TC best-track data from the U.S. Joint Typhoon warning centre.

The boreal summer is from May to October. All the datasets have been preprocessed so that the seasonal cycles are removed. The finite-domain wavenumber-frequency energy spectrum analysis[27], lead and lag regression analysis, Butterworth band-pass filter and other conventional diagnostic analysis of climate statistics are employed.

According to He et al.[28], the ISO and the tropical synoptic waves are represented by 20-70-day and 3-7-day bandpass-filtered data, respectively. Hereafter, the 20-70-day filtered outgoing longwave radiation anomalies (OLRA) are named ISO-OLRA and the 3-7-day filtered OLRA are recorded as TD-OLRA, and so forth.

The whole latent heat of water vapor $E=\int_{1000}^{300} Lq\mathrm{d}p$, where L is the latent heat of condensation, defined as L=(597.3-0.566 t)×4186.84 J/kg, t the air temperature, q the specific humidity.

In order to quantitatively indicate the strength of TC activity over the western north Pacific (WNP), the accumulated TC activity index (TAI) in the WNP (including South China Sea, north of the equator, west of 180° E) from 1979 to 2004 is specifically defined. The total 6-hourly records of TCs in every pentad, called pentad TAI, are calculated first, based on which the monthly TAI and yearly TAI are then calculated. The value of TAI is positively correlated with the TC activity in the WNP.

Figure 1 shows the yearly TAI in the boreal summer. It can be seen that the summertime TAI for 1979–2004 shows a remarkable interdecadal oscillation and TC activity is inactive during 1980s and from late 1990s to early 2000s. Based on the standardized TAI in the 25 years, the active (or inactive) TC years are distinguished by the value of TAI greater than 0.75 (or less than -0.75) standard deviation. The inactive years are 1981, 1983, 1986, 1988, 1998, 1999 and the active years are 1992, 1994, 1995, 1996, 1997 (Fig. 1). The mean TC number for the active year (inactive year) is 29.2 (21.5).

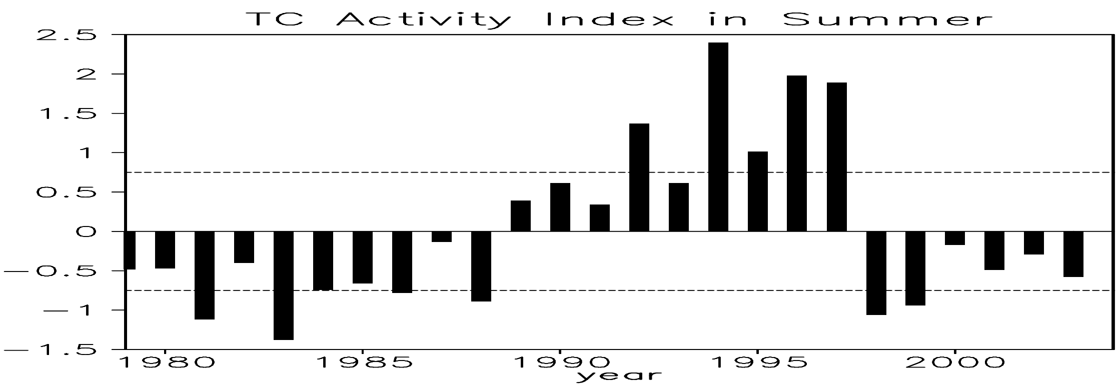

Fig. 1. The annual standardized accumulated TC activity index from 1979 to 2004 in the western North Pacific in boreal summer (the bar denotes the index value, and the two dashed lines are for 0.75 and -0.75 standard deviation, respectively).

3 CHARACTERISTICS OF REGIONAL LOW-FREQUENCY OSCILLATION

The ISO exhibits a zonal wave-number-1 propagation in different regions[1, 5-7]. Fig. 2 shows the finite-domain power spectrum difference between the average active years and inactive years over the different regions of the 10° S–30° N in Asia through the western Pacific (AWP). It can be seen that the eastward significant deviation region (shaded) is located within 20 latitudes off the equator in the AWP area, and the positive difference of the 30-60-day period energy spectrum suggests that the power of the eastward propagation along the equator with the 30-60-day period is stronger in the active years than that in the inactive years (Fig. 2a). The wave power of the eastward propagation with the 20-30-day period in the vicinity of 20° N is stronger in the active years than in the inactive years. As the westward propagation with the 20-40-day period is the major climate propagation characteristics in the area[28], the differences indicate that the westward propagation in the active years is weaker in contrast to that in the inactive years. It also can be seen in Fig. 2a that the power spectrum of the westward propagation with the 12-20-day period in 10–20° N is significantly weaker in the active years, corresponding to the enhanced eastward propagation.

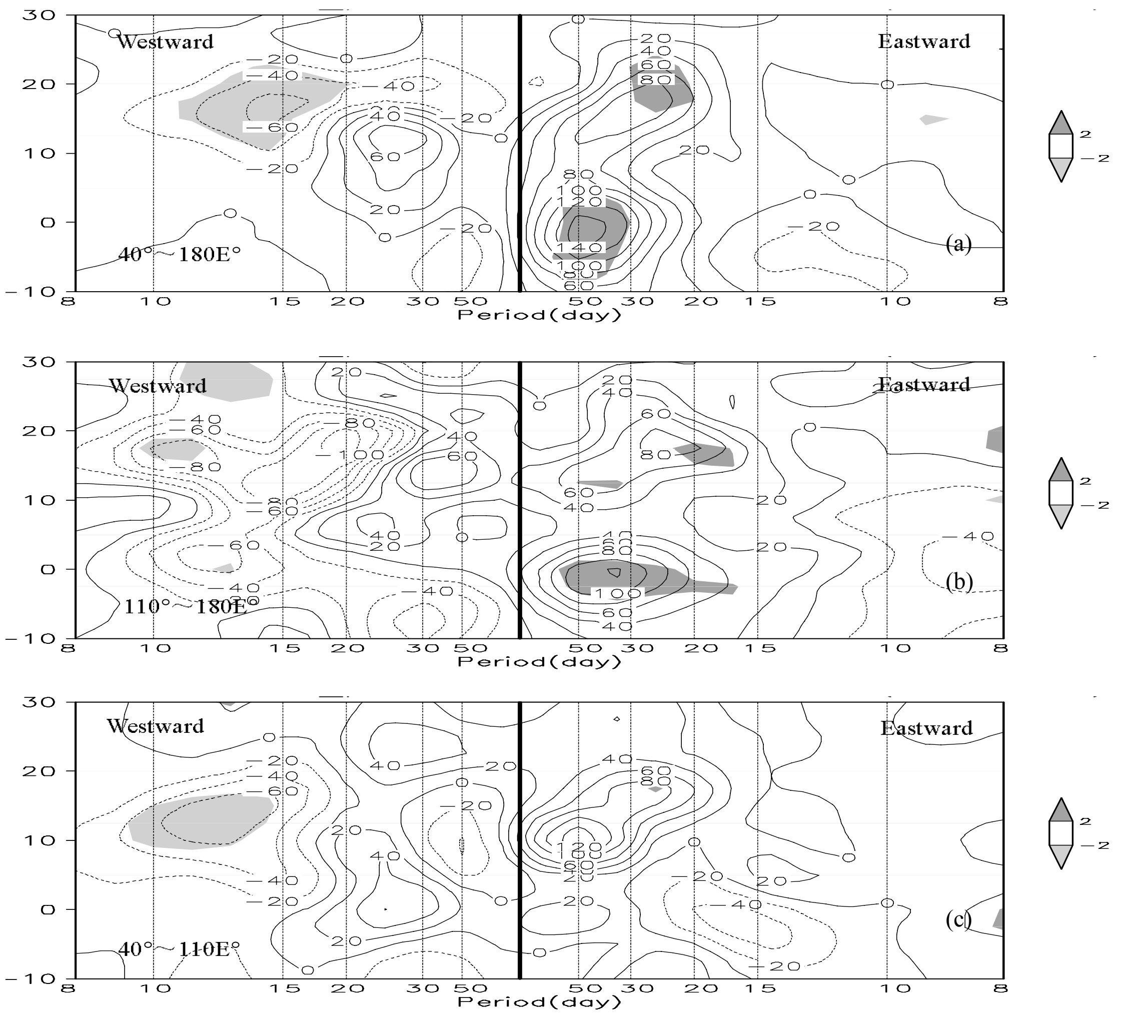

Fig. 2. The difference of power spectrum between active and inactive TC years in different regions in boreal summer (the mean of active years minus that of inactive years, the same below; the solid lines are for positive and the dashed for negative; confidence levels greater than 90% are shaded; a, b, c refer to 40–180° E, 110–180° E, and 40–110° E, respectively).

In the western Pacific region (110° E–180° , Fig. 2b), the characteristics of significant deviation between the active and inactive years are the same as those in the whole AWP region, i.e., the power of the eastward propagation along the equator with the 30-60-day period is stronger in the active year, while the significant shaded area is smaller than that in the whole AWP region. This suggests that not only the eastward propagation characteristics of disturbances along the equator but also the phase speeds of some disturbances are enhanced in the active year over the western Pacific. The westward 20-40-day period is dominant in the 10–20° N in the western Pacific region[28], though the power deviation of the westward waves between the active and inactive TC years is not significant at the 90% confidence level. In the Indian Ocean region (40–110° E, Fig. 2c), there is no significant deviation in the characteristics of the ISO eastward propagation between the active and inactive TC years, and the marked deviation is the decreasing power spectrum of the westward 10-15-day period waves, which belongs to the quasi-biweekly oscillation range, in the 10–20° N region.

4 COMPARISON OF PROPAGATION CHARACTERISTICS OF DIFFERENT

PHASE

4.1 *Low-level circulation features*

Figure 3 shows the mean ISO-OLRA standard deviation that reflects the main activity area and intensity of the summertime ISO convection. The intensity of ISO-OLRA is stronger in the active year than in the inactive year, and the range of the ISO-OLRA's high standard deviation (greater than 16 w/m^2) reaches the vicinity of 160° E. The value that is greater than 22 w/m^2 is mainly located in the South China Sea in the active TC years. The convective ISO is further eastward and the intensity is stronger over the western North Pacific in the active year.

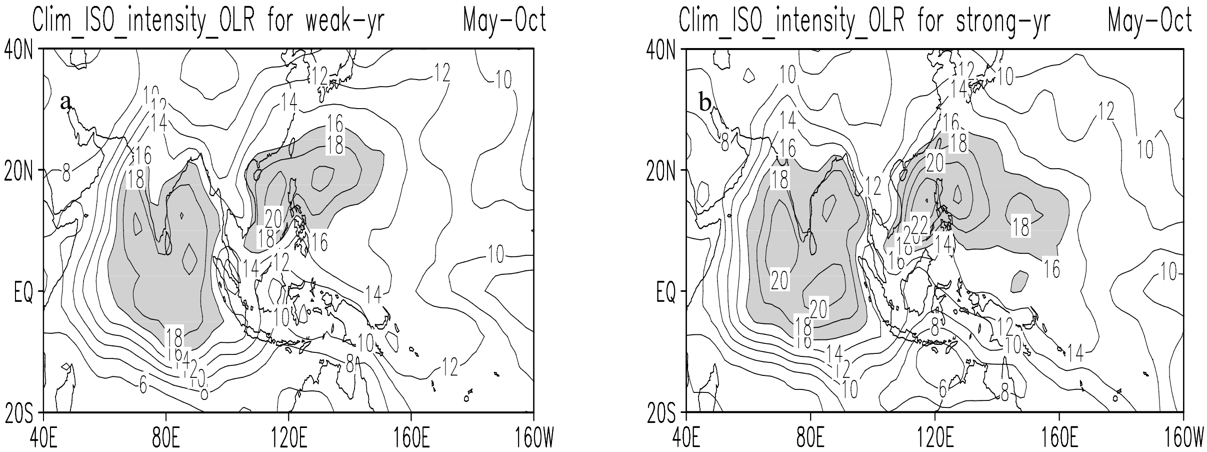

Fig. 3. The mean ISO-OLRA standardized deviation in active and inactive TC years in boreal summer (a: the inactive year; b: the active year; the strong convection zone greater than 16 w/m^2 is shaded; the contour interval is 2 w/m^2).

The key area is defined as (110–130° E, 10–20° N) where the strongest ISO convection is located (Fig. 3), and the average value of the ISO-OLRA of the key box represents the ISO convection intensity. The standardized daily time series of ISO intensity index in the active and inactive year are created, respectively. The ISO-filtered daily OLRA, 850-hPa stream function and TD-OLRA variance are obtained by the lag or lead regression results based on the daily ISO-OLRA standardized index in the active and inactive year, respectively. Fig. 4 shows the features of the two main phases of ISO in the active and inactive year, respectively. The TD-OLRA variance regression coefficient (thick lines) represents the active (suppressed) activity of the TD waves as the value is positive (negative). It shows that, regardless of active or inactive years, on day -15(the 15-day lead regression), the suppressed ISO convection in the WNP region coincides with the 850-hPa anticyclonic anomaly circulation and TD-OLRA variance negative anomalies, and the cyclonic circulation anomalies are located from the Indian Ocean to western Pacific near the equator, with the easterly anomalies to the southern side of the suppressed convection zone. On day 0, the deep convection is located between 10° N and 20° N over the Bay of Bengal to the WNP, with the 850-hPa cyclonic circulation coincided with positive TD-OLRA variance anomalies, and the westerly anomalies are located to the south of the strong convection. If the WNP region is taken as a standard, then the dry phase is on day -15 and the wet phase is on day 0, and these two phases are contrary to each other. The dry (wet) phase coincides with the low-level anticyclone (cyclone) anomalous circulation. The TD-OLRA regression variances coincide with the OLRA region (110–130° E, 10–20° N), reflecting the agreement between tropical synoptic waves and the ISO convection activities in the region. The negative OLRA regression values associated with the deep convection coincide with the positive TD-OLRA regression variance coefficient, suggesting that active ISO convection is accompanied by active tropical synoptic waves, which agrees with the previous studies[28, 29].

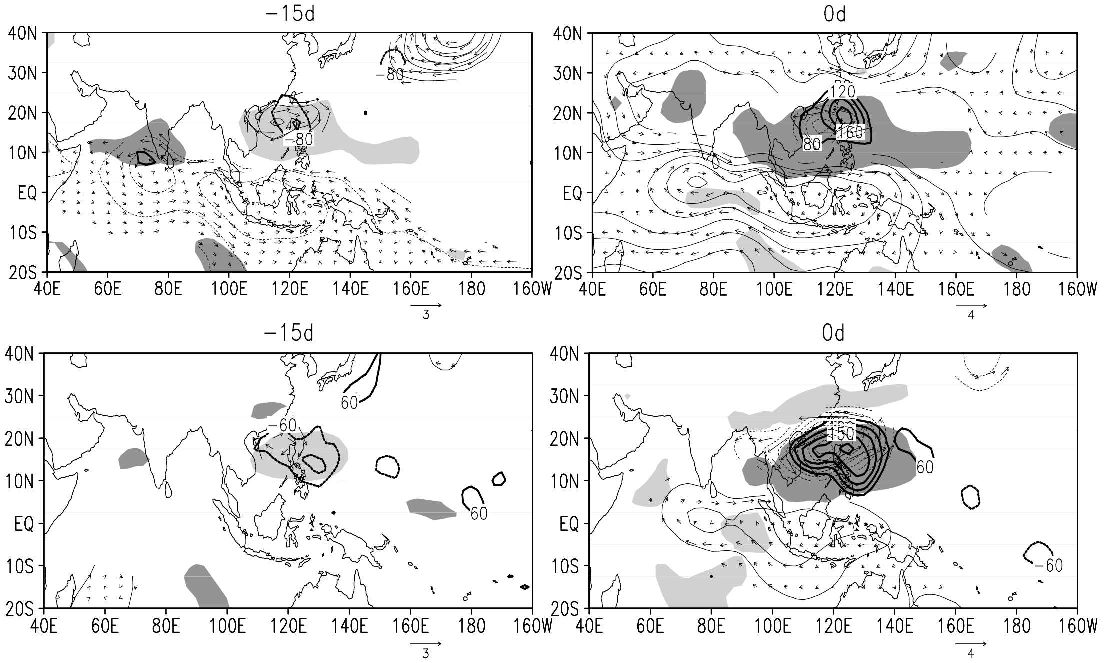

Fig. 4. The regressed OLRA (light shading is for positive and deep shading negative), 850-hPa streamfunction anomalies (shown by thin black contours; solid lines are for positive, dashed negative, at interval of 4×10^5 m^2/s), 850-hPa vortex wind (vector, m/s), TD-OLRA variance regression coefficient (shown by thick contours; solid lines are for positive, dashed negative, and the intervals in active and inactive years are 40 and 30 W^2/m^4, respectively) based on standardized ISO-OLRA index in active and inactive years. Significance levels greater 95% are plotted (upper panels: active years; lower panels: inactive years).

It is also shown from Fig. 4 that the main difference of the wet or dry phase mode between the active and inactive TC years is that the values of regression variables are greater in the active year. The standard intensity of OLRA in the key area (as indicated by the box) of the WNP region in the active year is 17.3 w/m^2, compared to only 14.0 w/m^2 in the inactive year. The ISO convection expands further east in the western Pacific in the active year.

The mean flow affects the ISO activities, and there are features of 30-60-day periods for the Indian Ocean and South China Sea to West Pacific summer monsoon, as well as the ITCZ[30, 31]. In the active TC years, the westerly anomalies in the wet phase in WNP suggests that this phase correlates with the active summer southwest monsoon, the eastward and northward extension of the southwest flow favor the northward movement of the monsoon trough, which will benefit the formation and development of TCs [21-23, 32], and the activities of tropical synoptic waves associated with the ISO are more active than those in the inactive year.

4.2 *Air-sea interactions in the ISO*

The convective condensation heating is an important feedback mechanism during the propagation of ISO, and the role of air-sea interaction is important to maintain the ISO, which relates to the physical variables such as SST, latent heat flux, shortwave radiative flux, moist static energy, etc.[13, 15, 19] There may be some differences between the active and inactive TC years in the intensity of the components of atmospheric and air-sea interactions during the ISO propagation process, causing the different characteristics of ISO propagation in the active and inactive year.

Figure 5 is a Hovmoeller diagram of the lag-regression physical components based on daily ISO-OLRA intensity indexes in active and inactive years, respectively. Due to the marked deviation of ISO propagation in active and inactive TC years located in the western Pacific region, the physical regression components are averaged over 110° to 180° E.

It can be seen from Figs. 5a & 5b that the physical components propagate poleward over the western Pacific, and the northward propagation is prominent. During the ISO convection cycle, the convection firstly occurs near the equator and propagates to 10° N on day -10. Then, the ascending flow and convection begins to strengthen, resulting in the release of latent heat of condensation. On day 0, the strongest center of convection superimposes with the biggest ascending velocity and the maximum latent heat of condensation with the center located in 10–20° N. The ISO convection can reach 30° N in the active year.

As shown in Figs. 5c & 5d, on day -20, there is a positive maximum value of DSWRF anomalies; on day -10, there are positive maximum surface temperature anomalies; on day 0, the maximum positive SLHF occurs when the most powerful convection develops, with the negative DSWRF reaching the maximum; on day +10, the negative maximum value of SKT anomalies appears, the SLHF anomalies become negative, the DSWRF is positive again. On day 20, the same maximum values of DSWRF as those on day -20 appear again, forming a complete ISO cycle.

Figure 5 describes the air-sea interaction processes of ISO. When the convection is suppressed, the SST increases as a result of the increased downward shortwave radiation. Water vapor is then transported from the ocean to the atmosphere, and the negative SLHF anomalies occur, followed by the increase of humidity. The unstable moist static energy is accumulated as a result of the sensible and latent heat. Finally, the convection generates and develops, releasing latent heat of condensation. At this time the values of SLHF turn into positive ones, indicating the moisture being transferred back into the ocean, which is similar to the process described by Wang and Xie[19], and Kemball-Cook and Wang[4]. The increased SST and moisture evaporation in the ocean occur in advance of the development of convection in the atmosphere, and in turn, the development of convection would influence the changes of SST and water vapor. The air-sea interaction processes are similar in both the active and inactive year, and the difference is merely the intensity of the physical variables. The energy of instability is more adequate in the active year than in the inactive year, favoring stronger convergence and more powerful development of convection, stronger latent heat of condensation and downward SLHF.

Significantly negative OLRA propagates eastward from the Arabian Sea, Indian Ocean to the vicinity of the dateline in both the equatorial region (Fig. 6a) and boreal subtropical region (Fig. 6b), suggesting stronger convection in the active year than that in the inactive year. It also coincides with the eastward propagation of the negative vertical velocity and positive latent heat energy of the whole troposphere, indicating that the latent heat release of the eastward propagating convection is also greater in the active year than in the inactive year. In the equatorial regions (Fig. 6a), the convection differences begin to propagate eastward from the 60–80° E Indian Ocean area on day -20, and become active in the western Pacific in day -5 to day 5 with the period being about 30–50 days. The enhanced eastward propagation in the subtropical region begins on day -15 in the vicinity of 40° E in the western African region, or in 60–80° E in the Arabian Sea and Indian Ocean areas. From day 0 to day 15, the standing waves enhance from the Indian Ocean to the western Pacific and the period of propagation shortens. These features are in consistency with the results of the power spectrum of ISO convection in the equatorial region and subtropical regions, i.e., the eastward 20-60-day period propagation is intensified in the active year. In the equatorial regions, active upward convection is located in the 60–80° E in the Arabian Sea and Indian Ocean as well as in the vicinity of the Philippines region, and the latent heat of condensation is also the strongest in these regions. In the subtropical region, the strongest convection regions are located in the 80–130° E and 140–160° E. The enhanced intensity of OLRA in the equatorial region is stronger than that in the subtropical region, and the difference between the active year and inactive year is greater than -10 w/m^2. However, compared to the inactive year, the released latent heat of condensation is greater in the subtropical region than that in the equatorial region, especially in the WNP. The values reach 40×10^5 J · hPa / kg or more in the active year.

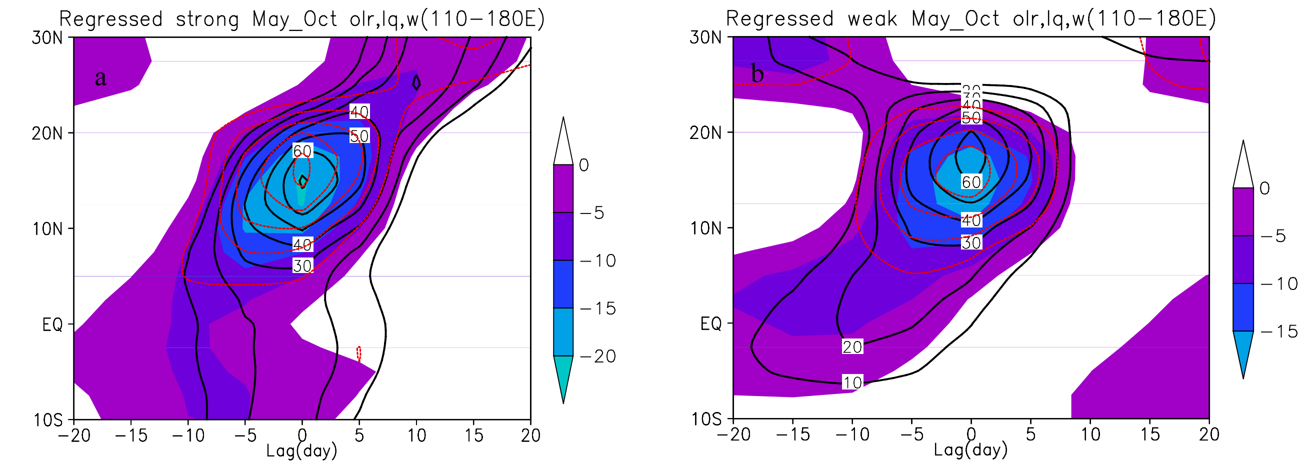

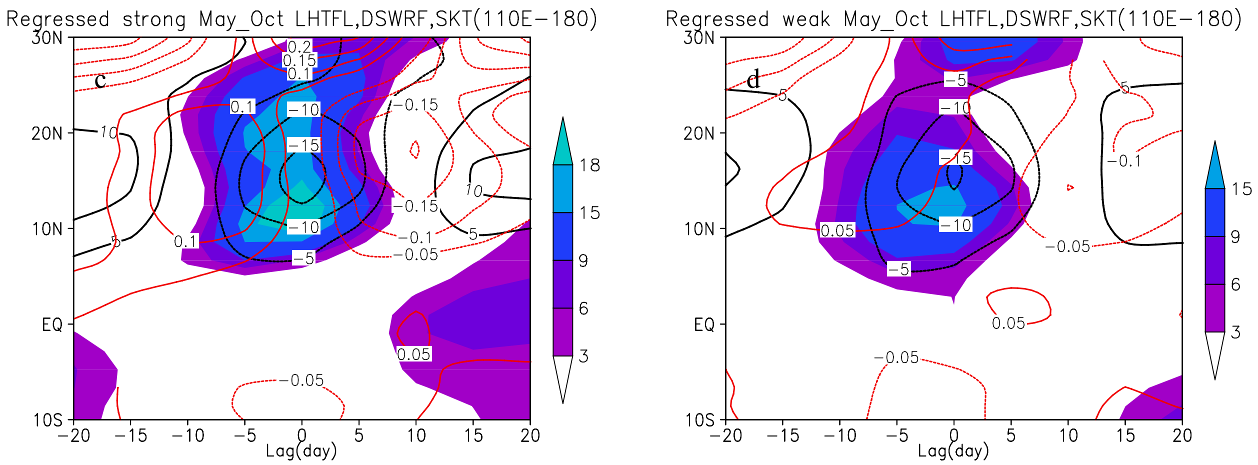

Fig. 5. The time-latitude Hovmoller plots of regressed variables based on ISO-OLRA intensity index in boreal summer in the TC active and inactive years (the color shading in (a) and (b) is for the negative OLRA, unit in w/m^2; the black solid line denotes positive anomalies of vertical integration of latent heat of condensation from 1000 hPa to 300 hPa, the interval is 10×10^5 J·hPa/kg; the red dashed line denotes the negative 500-hPa vertical velocity with intervals of 0.005 Pa/s; the color shading of (c) and (d) is for positive anomalies of SLHF, and the color scale denotes the value range, unit in w/m^2; the black lines denote the DSWRF anomalies, solid/dashed line for positive/negative value, the interval is 5 w/m^2, the zero line is omitted; the red line is the SKT anomalies, the interval is 0.05 °C; (a) and (c) are for the active year, and (b) and (d) for the inactive year).

No marked deviation of ISO propagation structure is identified, although there is significant difference in the propagation period (or phase speed). This may be related to various scale and intensity of condensation heat of convection for various TC activities in the WNP in different years. The CISK-Kelvin and CISK-Rossby theories can be used to explain low-frequency oscillations[12-19]. According to Liu et al.[17], when the condensation heating is considered, the frequency of the low-latitude atmospheric long-wave fluctuations is defined as:

$$\omega = \frac{(1-\frac{\eta_2}{2})kc_2}{-4m+1}, \ (m=0,1,2,\dots)$$

where η_2 is the parameter for the latent heat of condensation ($\eta_2 > 0$), $c_2 = \sqrt{\frac{2}{3}}N\Delta z$ (usually 24 m/s), N the Brunt-Vaisala frequency, Δz the interval of equal levels of the z-coordinate, $m = 0$ the CISK-Kelvin wave, and $m > 0$ the CISK-Rossby wave. The high-frequency Rossby wave is mainly active in the western Pacific[18, 19] when $\eta_2 > 2$, then $\omega > 0$, namely, the enhanced latent heat will favor the eastward propagation of CISK-Rossby wave, which can explain why the characteristics of eastward propagation of ISO are more significant in active TC years. The above analysis also shows that the heating intensity is stronger in the active year than in the inactive year, suggesting the modulation of latent heat of condensation released by TC convections may be responsible for different characteristics of ISO between the active and inactive TC years.

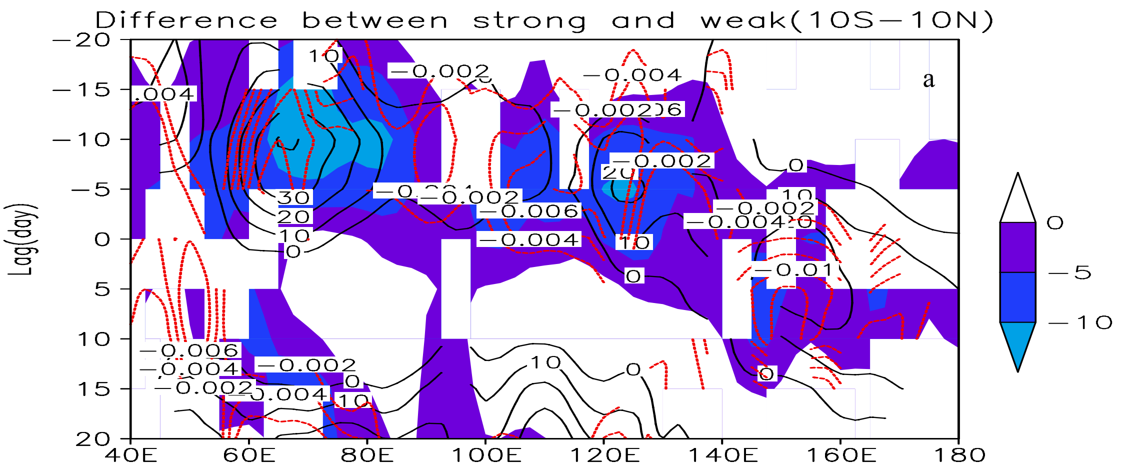

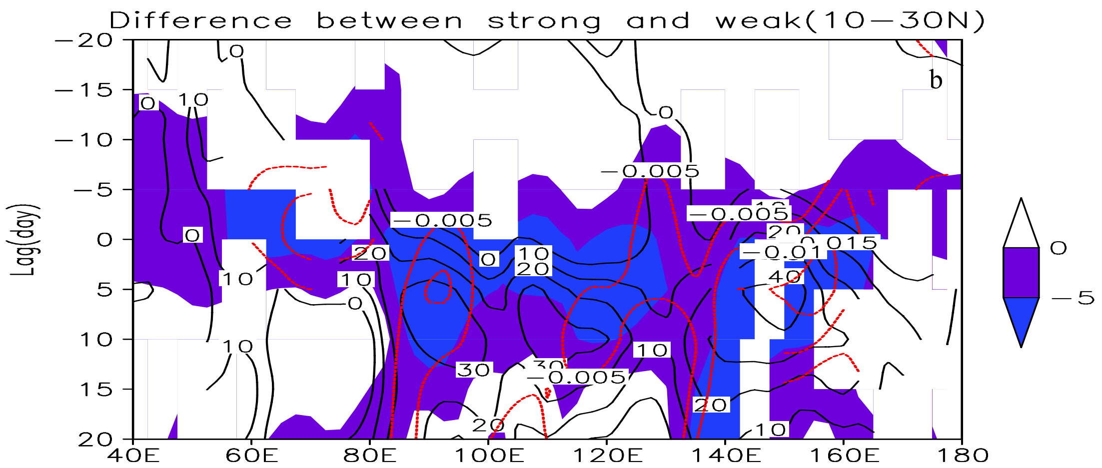

Fig. 6. The time-longitude Hovmoller plots of the difference of regressed variables between active and inactive TC years based on the ISO-OLRA intensity index in boreal summer (a: average in 10° S to 10° N; b: average in 10 to 30° N; negative OLRA is shaded, unit in w/m^2; the black lines denote the anomalies of the condensation latent heat of water vapor with intervals of 10×10^5 J·hPa /kg, the red dashed line denotes the negative vertical velocity at 500 hPa, the interval is 0.002 Pa /s for (a) and 0.005 Pa /s for (b)).

5 CONCLUSIONS

The difference of propagating characteristics and air-sea interaction process of boreal summer ISO over the AWP region between active and inactive years of TC activity are explored, and the major results are summarized as follows.

(1) The main difference of ISO propagation characteristics between active and inactive TC years is that the eastward 20-60-day period propagation along the equator is more significant in the active year. As the activity of 20-30-day period waves enhances, the phase speed of the waves propagating eastward along the equator increases in the western Pacific region. The western Pacific is the region where the propagation shows significant deviations, which closely relates to the TC activities. The ISO convection expands further east in the WNP in the active year.

(2) The south portion of ISO convection in the wet (dry) phase coincides with low-level westerly (easterly) anomalies in the WNP. The general circulation anomalies are more active and the convection expands further east in the active year. The enhanced ISO convection over WNP is consistent with the active status of tropical synoptic waves over the region.

(3) The enhanced downward short-wave radiation and increased sea surface temperature before the formation of strong convection favor the evaporation of moisture and the growth of unstable moist static energy, which then intensifies low-level convergence and upward convection development. In turn, the enhanced convection and release of latent heat are associated with the increase of SLHF and the decrease of DSWRF that the ocean obtains. When the intensity of convection reaches the maximum, the downward solar radiation is the minimum, resulting in the decrease of SKT and weakening of convection, which completes the cycle of ISO. The air-sea interaction is more active in the active year than in the inactive year.

It is also noticed that the difference in the strength of TC activity in the WNP between active and inactive years is closely associated with the various propagating characteristics of ISO convection and the ocean-atmosphere physical process. In other words, the activity of TCs may have feedback on the ISO. Although ISO modulates TC activities first[21-23, 32], the feedback of TC activities to ISO is not quite clear, which deserves to be further examined.

Acknowledgements**:** We sincerely thank NOAA-CIRES Climate Diagnostics Center for sharing the reanalysis data on the website: http://www.cdc.noaa.gov All figures in the present article are plotted using the software Grads.

REFERENCES:

[1] MADDEN R A, JULIAN P R. Observations of the 40-50-day tropical oscillation –A review [J]. Mon. Wea. Rev., 1994, 122(5): 814-837.
[2] ZHU B Z, WANG B. The 30-60-day convection seesaw between the tropical Indian and Western Pacific oceans [J]. J. Atmos. Sci., 1993, 50(2): 184-199.
[3] HSU H H, WENG C H. Northwestward propagation of the intraseasonal oscillation in the western north Pacific during the boreal summer: structure and mechanism [J]. J. Climate, 2001, 14(18): 3834-3849.
[4] KEMBALL-COOK S, WANG B. Equatorial waves and air–sea interaction in the boreal summer intraseasonal oscillation [J]. J. Climate, 2001, 14(13): 2923-2942.
[5] TENG H, WANG B. Interannual variations of the boreal summer intraseasonal oscillation in the Asian-Pacific region [J]. J. Climate, 2003, 16(22): 3572-3584.
[6] DONG M, ZHANG X, HE J. Tropical Intraseasonal Oscillation diagnosis of space-time characteristics (in Chinese)

[J]. Meteor. Mon., 2004, 62(6): 821-830.
[7] LIN A, LI T. Energy Spectrum characteristics of boreal summer intraseasonal oscillations: climatology and Variations during the ENSO developing and decaying phases [J]. J. Climate, 2008, 21(23): 6304-6320.
[8] HOLTON J R. On the frequency distribution of atmospheric Kelvin waves [J]. J. Atmos. Sci., 1973, 30(3): 499-501.
[9] LINDZEN R S. Wave-CISK in the tropics [J]. J. Atmos. Sci., 1974, 31(1): 156-179.
[10] LINDZEN RS . Wave-CISK and tropical spectra [J]. J. Atmos. Sci., 1974, 31(5): 1447-1449.
[11] CHANG C P. Viscous internal gravity waves and low-frequency oscillations in the tropics [J]. J. Atmos. Sci., 1977, 34(6): 901-910.
[12] YAMAGATA T, HAYASHI Y. A simple diagnostic model for the 30-50day oscillation in the tropics [J]. J. Meteor. Soc. Japan, 1984, 62(5): 709-717.
[13] LI Cong-yin. The activity of south Asia monsoon trough or ridge and tropical cyclone associated with mobile CISK wave(in Chinese) [J]. Sci. in China (Ser. B), 1985, 15(7): 667-674.
[14] LAU K M, PENG L. Origin of low-frequency (intraseasonal) oscillations in the tropical atmosphere. Part I: basic theory [J]. J. Atmos. Sci., 1987, 44(6): 950-972.
[15] CHANG C P, LIM H. Kelvin wave-CISK: A possible mechanism for 30-50d oscillation [J]. J. Atmos. Sci., 1988, 45(11): 1709-1720.
[16] MADDEN R A. Seasonal variations of the 40-50 day oscillation in the tropics [J]. J. Atmos. Sci., 1986, 43(24): 3138-3158.
[17] LIU S K, WANG J. Wave-CISK in a baroclinic semi-geostrophic model and low-frequency oscillations [J]. Meteor. Mon., 1992, 50(4): 393-402.
[18] WANG B, XIE X. A model for the boreal summer intraseasonal oscillation [J]. J. Atmos. Sci., 1997, 54(1): 72-86.
[19] WANG B, XIE X. Coupled modes of the warm pool climate system. Part I: The role of air–sea interaction in maintaining Madden–Julian oscillation [J]. J. Climate, 1998, 11(8): 2116-2135.
[20] HARTMANN D L, MICHELSEN M L, KLEIN S A. Seasonal variations of tropical intraseasonal oscillation: a 20-25-day oscillation in the Western Pacific [J]. J. Atmos. Sci., 1992, 49(14): 1277-1289.
[21] LIEBANN B B, HENDON H H, GLICK J D. The relationship between tropical cyclones of the western Pacific and Indian oceans and the Madden-Julian oscillation [J]. J. Meteor. Soc. Japan, 1994, 72(3): 401-411.
[22] ZHU C, NAKAZAWA T, LI J. Intraseasonal Oscillation in the Indian Ocean - Western Pacific of tropical depression / cyclone(in Chinese) [J]. Meteor. Mon., 2004, 62(1): 42-50.
[23] NAKAZAWA T. Madden-Julian oscillation activity and typhoon landfall on Japan in 2004 [J]. J. Meteor. Soc. Japan, 2006, 2: 136-139. doi:10.2151/sola.2006-035.
[24] HUANG Yong, LI Cong-yin, WANG Yin. Pacific ocean-atmosphere coupled mode and by the Pacific Northwest to the tropical cyclone frequency relationship (in Chinese) [J]. J. Trop. Meteor., 2009, 25(2): 169-174.
[25] SOBEL A H, CAMARGO S J. Influence of western North Pacific tropical cyclones on their environment [J]. J. Atmos. Sci., 2005, 62: 3396-3407.
[26] KALNAY E, COAUTHORS. The NCEP/NCAR 40-year reanalysis project [J]. Bull. Amer. Meteor. Soc., 1996, 77(3): 437-470.
[27] HAYASHI Y. Space–time spectral analysis and its applications to atmospheric waves [J]. J. Meteor. Soc. Japan, 1982, 60(1): 156-171.
[28] HE Jie-lin, WAN Qi-lin, GUAN Zao-yong, et al. On the characteristics of propagation of intraseasonal oscillations and their observed association with tropical synoptic waves in the Asian-western Pacific region in boreal summer [J]. J. Trop. Meteor., 2011, 17 (3): 248-256.
[29] STRAUB K H, KILADIS G N. Interactions between the boreal summer intraseasonal oscillation and higher-frequency tropical wave activity [J]. Mon. Wea. Rev., 2003, 131(5): 945-960.
[30] LIN Ai-lan, LIANG Jian-yin, LI Chun-hui. Summer monsoon intraseasonal oscillation spectrum convection variation [J]. J. Trop. Meteor., 2005, 21(5): 542-548 (in Chinese).
[31] LIU Ge, SUN Su-qing, ZHANG Qing-yun, et al. ITCZ and its seasonal tropical cyclone within the oscillating relationship between the occurrence of phase [J]. Chin. J. Atmos. Sci., 2009, 33(4): 879-889.
[32] CHEN Guang-hua, HUANG Rong-hui. Dynamical effects of low frequency oscillation on tropical cyclogenesis over the western North Pacific and the physical mechanisms [J]. Chin. J. Atmos. Sci., 2009, 33(2): 205-214.

Citation: HE Jie-lin, WAN Qi-lin, GUAN Zhao-yong et al. Intraseasonal oscillations in Asia to western Pacific region in boreal summer: Contrastive analysis for active and inactive years of tropical cyclones. ***J. Trop. Meteor.***, 2011, 17(4): 326-334.